

Challenges in multiphysics modeling of dual-band HgCdTe infrared detectors

M. Vallone*, M. Goano*[†], A. Tibaldi*[†], S. Hanna[‡], D. Eich[‡], A. Sieck[‡], H. Figgemeier[‡]
 G. Ghione*, F. Bertazzi*[†],

* Dipartimento di Elettronica e Telecomunicazioni, Politecnico di Torino, corso Duca degli Abruzzi 24, 10129 Torino, Italy

[‡] AIM Infrarot-Module GmbH, Theresienstraße 2, D-74072 Heilbronn, Germany

[†] IEIIT-CNR, corso Duca degli Abruzzi 24, 10129 Torino, Italy

E-mail: michele.goano@polito.it

Abstract—We present three-dimensional simulations of HgCdTe-based focal plane arrays (FPAs) with two-color and dual-band sequential infrared pixels having realistic truncated-pyramid shape taking into account the presence of compositionally-graded transition layers. Simulations emphasize the importance of a full-wave approach to the electromagnetic problem, and the evaluations of the optical and diffusive contribution to inter-pixel crosstalk indicate the effectiveness of deep trenches to prevent diffusive crosstalk in both wavebands.

I. INTRODUCTION

Multispectral capability across infrared (IR) bands is a central requirement for third generation, large format infrared (IR) focal plane array (FPA) detectors. The outstanding properties of $\text{Hg}_{1-x}\text{Cd}_x\text{Te}$ allow to fabricate large format dual-band or two-color IR FPA detectors. Each pixel includes two stacked p - n absorbers, i.e., two back-to-back p - n photodiodes with different cut-off wavelength, separated by a thin, wide bandgap layer acting as barrier, and a single bias contact [1]–[3].

After validating in Section II the computational method against literature experimental data, we simulated in Section III a dual-band MWIR-LWIR [2] detector operating at $T = 230$ K, considering a 5×5 miniarray of pixels illuminated by a narrow Gaussian beam focused on its central pixel (CP), obtaining useful indications about the optimal bias point and effect of pixel geometry on the spectral quantum efficiency (QE) and inter-pixel crosstalk.

II. MODELING METHOD AND ITS VALIDATION

The simulations have been carried out with a commercial simulator with customizable material library [5], including an electromagnetic solver (EMW) based on the Finite Difference Time Domain (FDTD) method [6], and an electron transport solver (Sentaurus Device), here employed in the drift-diffusion approximation. EMW calculates the optical carrier generation rate distribution G_{opt} into the pixels, treated as a source term for the carrier continuity equations. The resulting photocurrent provides the spectral QE and inter-pixel crosstalk, calculated as defined e.g. in [7].

The HgCdTe properties were described through the models reported in [8], taking into account the composition, doping, and temperature dependence of the HgCdTe alloy. Shockley-Read-Hall (SRH) recombination processes were modeled as in

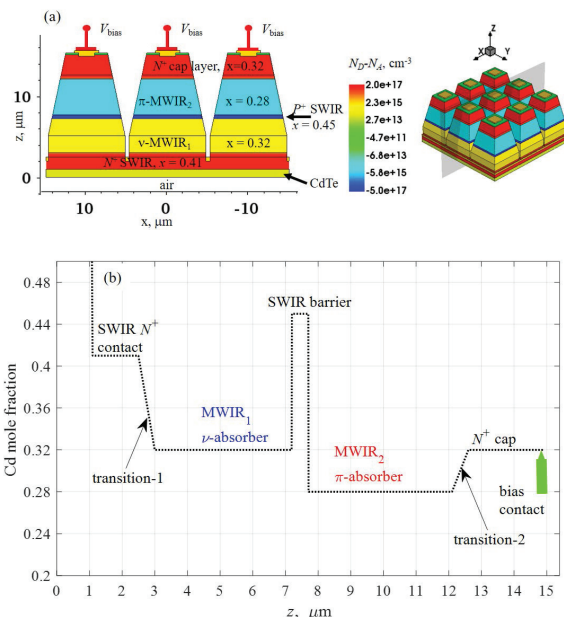


Fig. 1. (a) 3D MWIR₁-MWIR₂ 3 × 3 miniarray inspired by [4], with (b) its composition profile along z .

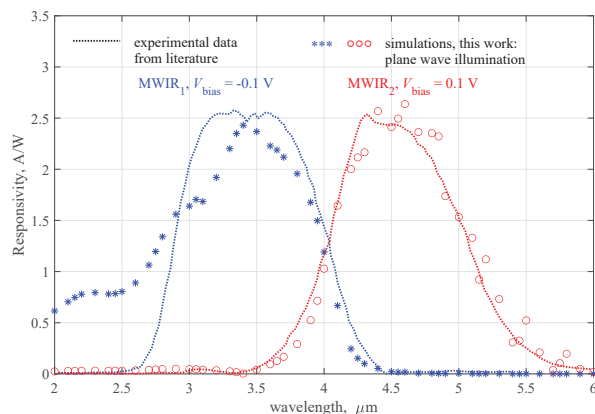


Fig. 2. 3D MWIR₁-MWIR₂ simulated spectral responsivity for plane wave illumination (symbols) compared with the experimental values from [4, Fig. 2].

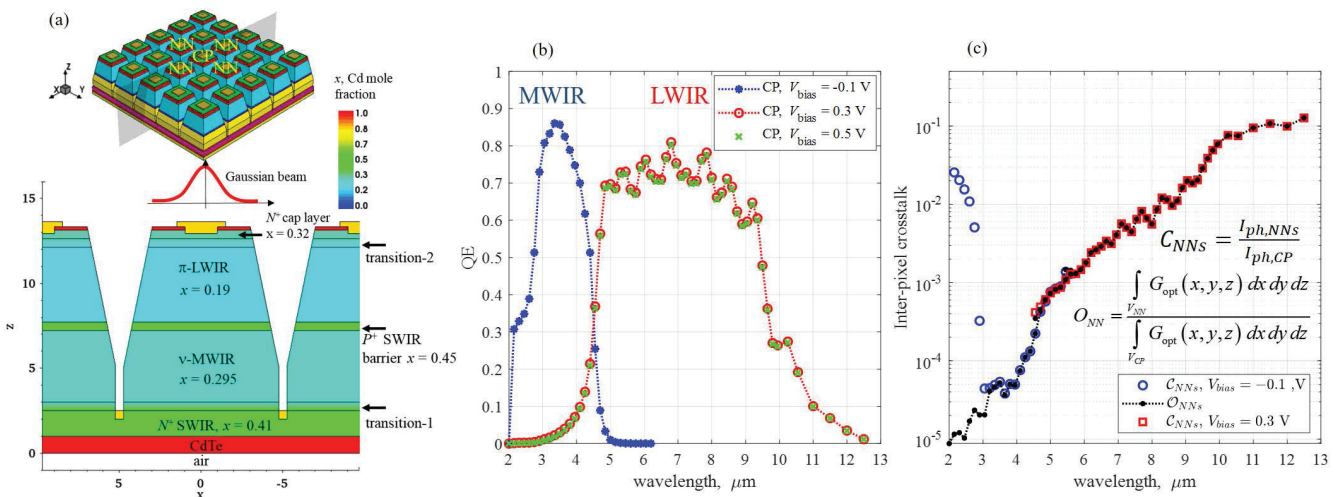


Fig. 3. (a) The simulated dual-band 5×5 MWIR-LWIR miniarray, with the central pixel (CP) and the nearest neighboring pixels (NNs). (b) Simulated spectral QE (MWIR: blue stars; LWIR: red circles and green crosses) for Gaussian beam illumination on the CP, and (c) inter-pixel crosstalk.

[9] considering a lifetime around $100 \mu\text{s}$. Fermi-Dirac statistics and incomplete dopant ionization were taken into account.

In order to validate the calculation method on experimental data, we simulated the 3×3 MWIR₁-MWIR₂ miniarray shown in Fig. 1(a,b), where the $\text{Hg}_{1-x}\text{Cd}_x\text{Te}$ compositional profile and the doping scheme along the growth direction z was kept as similar as possible to the structure from Ref. [4]. The pixels are defined by triangular trenches as truncated pyramids with $10 \mu\text{m}$ wide square base, and the presence of compositionally graded, transition layers was treated as in [10].

In Fig. 2 the simulated spectral responsivity for plane wave illumination shows satisfactory agreement with the experimental curves obtained from [4], plotted on the same figure for comparison (no parameters or normalization constants have been employed to fit simulations and experimental data).

III. DUAL-BAND MWIR-LWIR DETECTOR

After this validation step, we considered a 5×5 MWIR-LWIR miniarray (see Fig. 3(a)) illuminated from below by a narrow Gaussian beam, with the beam axis orthogonal to the detector horizontal plane xy , centered on the miniarray CP and focused on the illuminated face. The dopant concentrations in all the layers are the same as for the MWIR₁-MWIR₂ detector, as well as the pixel pitch and sidewalls angle.

A parametric simulation campaign provided the best P^+ -SWIR barrier composition ($x = 0.45$) and the optimal bias point for each waveband (-0.1 V and 0.3 V to select respectively the MWIR and LWIR band). In Fig. 3(b,c) the spectral QE and interpixel crosstalk are shown (see crosstalk definitions and extensive discussions in [7], [8], [11]–[13]). Beside describing the effects of multiple internal reflections due to metallization and pyramidal pixel sidewalls, simulations demonstrate the key role of the deep trenches in preventing the diffusive crosstalk in both wavebands. Simulations also indicate the presence of significant optical crosstalk, rapidly

growing with increasing wavelength, whose reduction possibly requires the optimization of the pixel shape.

REFERENCES

- [1] M. A. Kinch, “Fundamental physics of infrared detector materials,” *J. Electron. Mater.*, vol. 29, no. 6, pp. 809–817, 2000.
- [2] P. Martyniuk, J. Antoszewski, M. Martyniuk, L. Faraone, and A. Rogalski, “New concepts in infrared photodetector designs,” *Appl. Phys. Rev.*, vol. 1, p. 041102, 2014.
- [3] D. Eich, C. Ames, R. Breiter, H. Figgemeier, S. Hanna, H. Lutz, K. Józwiowski, T. Schallenberg, A. Sieck, and J. Wenish, “MCT-based high performance bispectral detectors by AIM,” *J. Electron. Mater.*, vol. 48, no. 10, pp. 6074–6083, 2019.
- [4] M. Kopytko, W. Gawron, A. Kębłowski, D. Stepieć, P. Martyniuk, and K. Józwiowski, “Numerical analysis of HgCdTe dual-band infrared detector,” *Opt. Quantum Electron.*, vol. 51, p. 62, 2019.
- [5] *Sentaurus Device User Guide. Version N-2017.09*, Synopsys, Inc., Mountain View, CA, Sep. 2017.
- [6] J.-P. Berenger, “A perfectly matched layer for the absorption of electromagnetic waves,” *J. Comp. Phys.*, vol. 114, no. 2, pp. 185–200, 1994.
- [7] M. Vallone, M. Goano, F. Bertazzi, G. Ghione, S. Hanna, D. Eich, A. Sieck, and H. Figgemeier, “Constraints and performance tradeoffs in Auger-suppressed HgCdTe focal plane arrays,” *Appl. Opt.*, vol. 59, no. 17, pp. E1–E8, 2020.
- [8] M. Vallone, M. Goano, F. Bertazzi, G. Ghione, W. Schirmacher, S. Hanna, and H. Figgemeier, “Simulation of small-pitch HgCdTe photodetectors,” *J. Electron. Mater.*, vol. 46, no. 9, pp. 5458–5470, 2017.
- [9] M. Vallone, M. Mandurrino, M. Goano, F. Bertazzi, G. Ghione, W. Schirmacher, S. Hanna, and H. Figgemeier, “Numerical modeling of SRH and tunneling mechanisms in high-operating-temperature MWIR HgCdTe photodetectors,” *J. Electron. Mater.*, vol. 44, no. 9, pp. 3056–3063, 2015.
- [10] M. Vallone, M. Goano, F. Bertazzi, G. Ghione, S. Hanna, D. Eich, and H. Figgemeier, “FDTD simulation of compositionally graded HgCdTe photodetectors,” *Infrared Phys. Tech.*, vol. 97, pp. 203–209, 2019.
- [11] B. Pinkie and E. Bellotti, “Numerical simulation of spatial and spectral crosstalk in two-color MWIR/LWIR HgCdTe infrared detector arrays,” *J. Electron. Mater.*, vol. 42, no. 11, pp. 3080–3089, 2013.
- [12] M. Vallone, M. Goano, F. Bertazzi, G. Ghione, S. Hanna, D. Eich, and H. Figgemeier, “Diffusive-probabilistic model for inter-pixel crosstalk in HgCdTe focal plane arrays,” *IEEE J. Electron Devices Soc.*, vol. 6, no. 1, pp. 664–673, 2018.
- [13] M. Vallone, M. Goano, F. Bertazzi, G. Ghione, S. Hanna, D. Eich, and H. Figgemeier, “Reducing inter-pixel crosstalk in HgCdTe detectors,” *Opt. Quantum Electron.*, vol. 52, no. 1, p. 25, 2020.